Sixth International Symposium on Turbulence and Shear Flow Phenomena
Seoul, Korea, 22-24 June 2009

TRANSPORT FEATURES INSIDE A THERMALLY FORCED CONVECTIVE BOUNDARY LAYER THROUGH 3D PTV AND TEMPERATURE MEASUREMENTS.

Valentina Dore
Department of Hydraulics, Transportations and Roads,
Sapienza University of Rome,
Via Eudossiana 18, 00184 Rome (Italy)
valentina.dore@uniroma1.it

Monica Moroni
Department of Hydraulics, Transportations and Roads,
Sapienza University of Rome,
Via Eudossiana 18, 00184 Rome (Italy)
monica.moroni@uniroma1.it

Antonio Cenedese
Department of Hydraulics, Transportations and Roads,
Sapienza University of Rome,
Via Eudossiana 18, 00184 Rome (Italy)
Antonio.Cenedese@uniroma1.it

ABSTRACT

A deeper insight into the dynamics of the convective boundary layer seems to be necessary for environmental purposes, as water or air quality monitoring in the upper oceans and lakes or in the lower troposphere. Transport and mixing features of stratified fluids while free convection occurs, due to the onset of thermal instability, are investigated by means of a laboratory model. Experiments are run in a tank filled with stably stratified distilled water and subjected to heating from below. The equipment is well designed for simultaneously providing temperatures, through thermocouples, and Lagrangian particle trajectories by using a fully three dimensional image analysis technique (3D Particle Tracking Velocimetry). The main goal in the experiment is predicting the spatial extension of the mixing region as a function of initial and boundary conditions. The mixing layer height is detected by employing temperature data and statistics of the velocity field, i.e. the vertical velocity component standard deviation. Finally, a more detailed description of transport and mixing from a non-local Lagrangian point of view is obtained through the transilient turbulence approach, resulting in the estimation of the transilient matrix, where each element represents the fraction of fluid moved by turbulence from one layer to another the domain has been previously divided in.

INTRODUCTION

Free thermal convection refers to the motion of vertical turbulent plumes or domes. It can occur when, an initially in-rest, density stratified fluid is submitted to buoyancy forces, caused by a permanent perturbation associated to a heat transfer mechanism. When a fluid, in equilibrium, is stably stratified the external forcing can produce an unstable configuration ensuing internal waves formation and increasing in amplitude, and, if it has strength enough, it can definitely erode the stratification, involving an increasing thickness of fluid volume. The entrainment phenomenon justifies the penetrative feature of convection and causes the growth of a convective boundary layer of well mixed fluid (Convective Mixing Layer or CML) against the adjacent stably stratified region.

The motivations of the research are mostly related to its connections to environmental topics. In nature, the dynamics of penetrative convection influences the transport and mixing features of stratified fluids, playing a fundamental role in characterizing and forecasting the distribution of chemical species, with implication for water or air quality in the upper oceans and lakes or in the lower troposphere. In most lakes, turbulent convective flow can be observed when the free surface becomes cooler than the underlying waters, eroding the stable stratification on a daily or seasonal time scale (Imberger and Ivey, 1991); this mechanism is fundamental to allow the water turnover, the redistribution of oxygen and nutrients and to avoid eutrofization. In the ocean under calm conditions, the upper twenty or thirty meters usually exhibit a continuous, moderately stable density distribution. When wind begins to blow over the surface, turbulence in the water is generated both by shear and sporadic breaking waves. With time, the turbulent layer becomes deeper as a result of the

entrainment and erosion of the underlying denser water. Because of the relatively rapid mixing, the density distribution is approximately uniform in the upper layer, and the entrainment takes place across the interface between the turbulent and stable fluids (Kato, H and Phillips, 1969). The persistence of sea ecosystems, and also coastal human activities, highly depends on the preservation of this delicate equilibrium. An analogous phenomenon is observed in the atmosphere when surface heating due to solar radiation results in a growing unstable layer adjacent to the ground which replaces a nocturnal inversion from below. In this case, the initially stable environment near the ground is affected by convection, and full interaction between the two regions occurs (Deardorff, 1979; Stull, 1988). The pollutants, released inside the mixing layer mainly by human activities, remain confined inside it; forecasting the dispersion of harmful contaminants in the lower troposphere is essential for the safety of populations living close to urban or industrial areas. On a larger scale, these investigations can have implications for climate change predictions if the fate of greenhouse gases is evaluated. In lakes and oceans, domes with large downward velocities are originating at the free surface, balanced by ascending domes with lower velocity but larger area. In the atmosphere, convection is characterized by relatively narrow plumes in the form of domes of rising horizontal surfaces balanced by larger regions of descending motion. Resulting oscillatory movements (internal waves) generated within the stable layer take place at or below the Brunt-Väissälä frequency which is related to the vertical temperature gradient. Penetrative convection also occurs in stars (Miesch et al., 2000). Stars of mass less than approximately one solar mass present a radiative core and a convective envelope; more massive stars have a convective core and a radiative envelope. Turbulent motion in the convective zone may penetrate into the stably stratified radiative regions. The amount of materials being mixed due to penetrative convection is a crucial ingredient in stellar evolution theories with important implications in astrophysics.

When studying turbulent convective phenomenon, dispersion is mostly due to transport by large organized structures while molecular diffusion can be neglected. The knowledge of the horizontal and vertical extension of the structures dominating the flow field appears to be mandatory. In order to better understanding and likely describing the evolution of turbulent structures inside the convective layer, a fully three dimensional experimental technique is required.

EXPERIMENTAL MODEL

The model used for laboratory experiments is a $0.40\times0.40\times0.41$ m^3 glass tank (Figure 1). The working fluid is distilled water. Pollen particles of about 80 μm diameter are used as the neutrally buoyant tracer. A stable stratification, e.g. a positive vertical temperature gradient, is generated, during filling the test section, by means of two connected tanks. After being stratified, the chamber is heated from below, to simulate the solar radiation effects and to trigger penetrative convection.

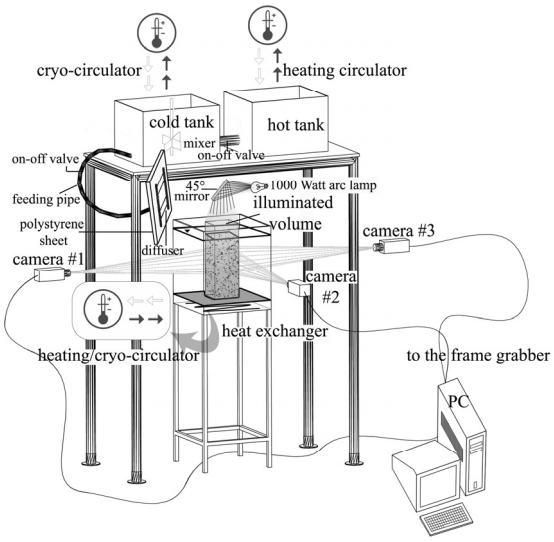

Figure 1. Sketch of experimental set up

The combined use of a vertical array of thermocouples and 3D-PTV allows, simultaneously, profiling temperature and computing 3D velocity components. Images of the well reflecting tracer particles have been recorded using a stereoscopic system of three monochrome 8-bit CCD cameras with a time resolution of 25 fps, focused on the domain ($0.15\times0.15\times0.20$ m^3 sized). The measuring volume has been illuminated by a high power (1000 Watt) arc lamp. A physically based photogrammetric calibration of the stereoscopic arrangement has been employed and its accuracy tested. The effects of multimedia geometry on calibration parameters have also been taken into account (Dore et al. 2009a).

Feature of Experiments

Two experiments are presented here. Their main features are reported in Table 1. Exp #1 presents a temperature gradient (γ) larger than exp #2 and a cooler initial temperature at the bottom (T_{b0}). The final value of temperature reached at the test section bottom due to heating is the same for both the experiments.

Table 1: Feature of experiments.

Exp #	T_{b0}	T_{bc}	$\gamma = (\partial\overline{T}/\partial z)$
	K	K	K/m
1	286.65	308.15	101.16
2	293.12	308.15	55.35

Figure 2a shows the initial and stable temperature stratifications for both the experiments. The measured profiles overlay to a linear interpolation that is very close to the experimental data in both cases. When heating from below begins, the temperature profile changes with time as the phenomenon evolves (Figure 2b and 2c).

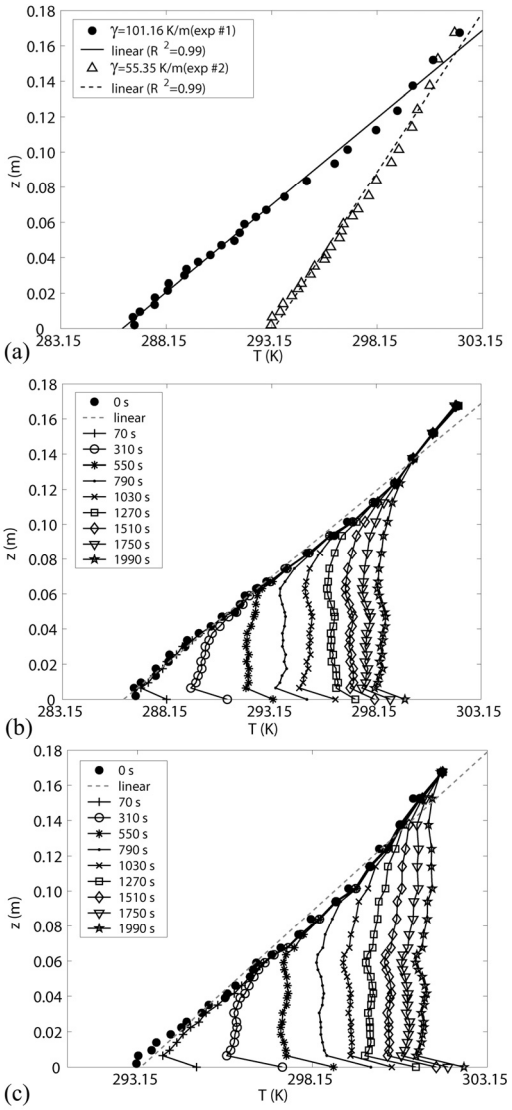

Figure 2. Temperature profiles: (a) initial conditions before heating starts; (b) time evolution during experiment #1; (c) time evolution during experiment #2.

Three regions characterize each profile from bottom to top:

- the Surface Layer presents a negative gradient proving that an unstable condition acts as a driving force for the onset of convection;
- the Convective Mixing Layer has a relatively uniform temperature $\overline{T}(t)$ due to turbulence;
- the Stable Layer presents a temperature profile which is not noticeably affected by the growing mixing layer and maintains the initial stratification.

Each temperature profile is associated with a time given in the legend even though it was obtained through averaging temperature data acquired for 20 seconds at each thermocouple location.

A photogrammetric 3D-PTV technique has been applied on the images acquired by means of the calibrated stereoscopic system.

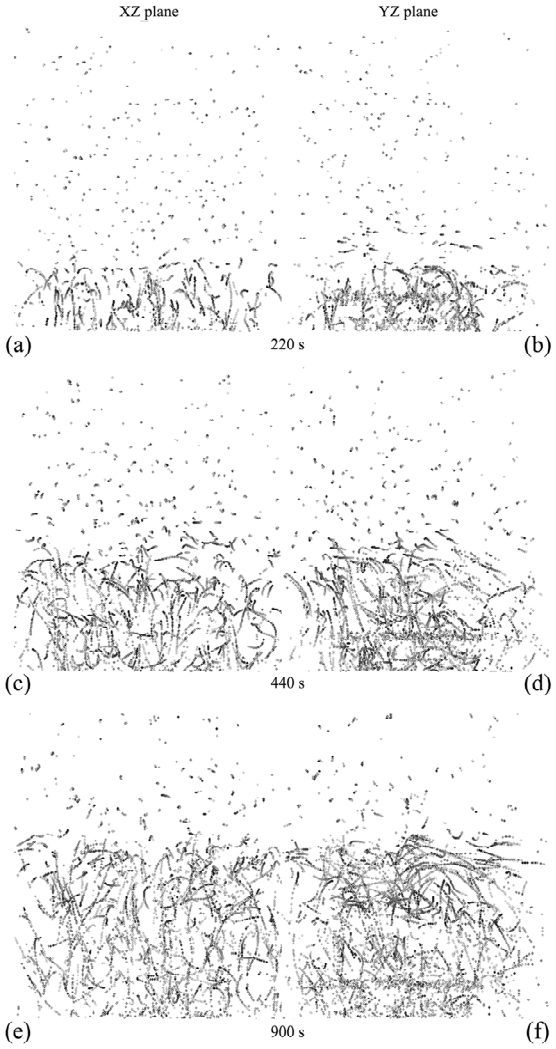

Figure 3. Projections on the XZ plane (a,c,e) and YZ plane (b,d,f) of matched centroids after 220 s (a,b), 440 s (c,d), 900 s (e,f) from the beginning of experiment #1. In both pictures, 50 s are overlaid and dark colour refers to later times (exp#1 of Table 1).

The combination of image and object space based information is employed to establish the spatio-temporal correspondences between tracer particle position of consecutive time steps, resulting in the reconstruction of 3D trajectories.The performance of the matching procedure has been evaluated through synthetic generated trajectories. Sensitivity tests on particle density and errors in calibration parameters have been also carried on (Dore et al., 2009a). Figure 12 shows matched centroids projected on the XZ plane (a,c,e) and the YZ plane (b,d,f) inside both the stable and the unstable layers after 220 s, 440 s and 900 s from the beginning of experiment #1 and tracked for at least 50 seconds. Darker colours have been linked to later times, while lighter colours to earlier times. From both projections it can be clearly seen that the turbulent region below is moving upward against the almost quiet stable layer. The 3D-PTV procedure is suitable for reconstructing the

displacement field (i.e. particle trajectories) in both the mixing and the stable layers.

DATA PROCESSING

The height of mixing layer, z_i, is comparable with the domes vertical dimension. Two methods are proposed and compared in order to compute the mixing layer upper limit: the first is based on temperature profiles and the second on velocity data.

Starting from the observation of profiles in Figures 2b and 2c we can assign z_i to the height where the uniform temperature region of each profile intersects the initial stratification line of slope $1/\gamma$. Thus, knowing the mean temperature within the mixing layer, the height can be computed as:

$$z_i(t) = \frac{1}{\gamma}(\overline{T}(t) - T_{b0}) \qquad (1)$$

Theoretically, the upper limit of the convective zone and the mixing layer height do not coincide exactly, and the temperature profile should exhibit an interface layer, called entrainment zone, where the temperature homogeneity overcomes the initial stratification line. The vertical extension of the entrainment zone is greater for lower initial stratification gradients. In our case, for both experiments the temperature gradient is so great that the entrainment interface can be neglected and equation (1) can be used to find the mixing layer height.

The mixing layer height can be evaluated with a given frequency (anyway less than 25 Hz, the largest frame rate for image acquisition) starting from velocity data by dividing the domain into layers and computing the vertical velocity standard deviation profiles (the horizontal homogeneity and isotropy assumption allows averaging velocity data in each layer over a chosen time interval).

As one can clearly see from Figure 4, the mixing layer region is characterized by values of the standard deviation of the vertical velocity greater than the stable layer, due to the onset of convection. For earlier times, the standard deviation is small everywhere, while, as time goes on, the standard deviation will increase in magnitude and cover an increasing portion of the fluid. This is a reflection of the growing mixing layer characterized by large fluctuations of the velocity about the mean value**.**

For each profile we find the height where the standard deviation became, after the peak, 30% of the maximum value and the profile slopes are still gentle, thus the z_i will be:

$$z_i(t) = \frac{1}{k} z_{30\%}(t) \qquad (2)$$

where $z_{30\%}(t)$ is the height associated to the standard deviation equal to 30% of the maximum value and k=0.7 is a constant empirically determined by using a larger set of experiments and findings of Cenedese and Querzoli (1994).

As we know the upper limit of the convective region acts as a barrier for the dispersion of a tracer inside the stable layer and consequently a scalar, like a pollutant, released inside the mixing layer remains confined inside it. On the other side, a downward transport exists from the stable to the mixing layer due to entrainment.

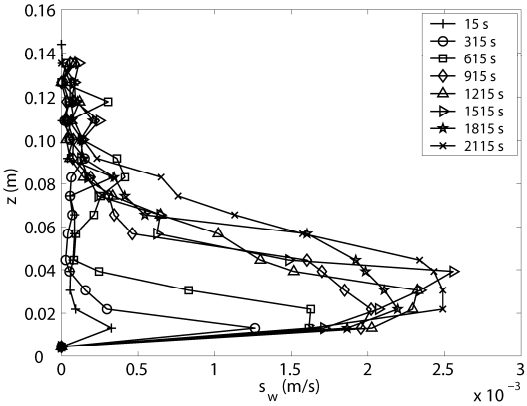

Figure 4. Standard deviation profiles of vertical velocity for experiment #1

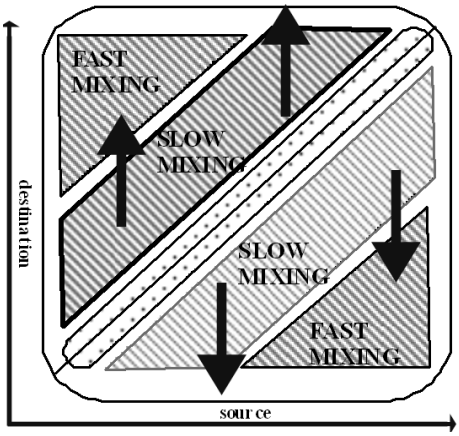

Figure 5. Physical meaning of elements throughout the transilient matrix

Starting from the point that dispersion phenomena in the mixing layer are non local, the classical approach based on local closure leading to the advection dispersion equation (ADE) is not suitable in this case and a non local description of turbulent transport is necessary. The non-local theory assumes that mixing between heights with finite separation can occur directly by fluid parcel movement, associated with coherent structures of a variety of size. A way of dealing with non-local transport is through the Lagrangian transilient matrix approach (Stull,1988). Employing a discretization of the domain in a series of N homogeneous horizontal layers (each identified by an index i), and assuming that each particle can randomly move among layers driven by turbulence, we can introduce the conditional probability $p_{ij}(t, \Delta t)$ that a particle belonging to a source layer j at time t moves to the destination i during a time interval Δt. The terms $p_{ij}(t, \Delta t)$, positive and less than 1, form a square matrix, called transilient matrix, where the row index i refers to the destination layer and the column index j refers to the source layer. Each element of the matrix is equal to the fraction of fluid transported by turbulent mixing from j to i during the time interval Δt. Assuming that transported fluid parcels carry their original features of heat, moisture, tracers, and momentum components and they remain constant on average along a trajectory, we can map the spatial distribution of whatever scalar at a certain time through a simple matrix multiplication:

$$C(t+\Delta t)=P(t,\Delta t)\,C(t) \qquad (3)$$

where C is an N-element column vector describing the state of each layer in terms of whatever scalar and P is the NxN transilient matrix. From a physical point of view a full transilient matrix holds information on the mixing process ranging from the smallest scales resolved by the grid spacing to the largest ones allowed by the domain. It includes the small eddy effects as well as the K-theory plus the medium and large advective-like coherent structure effects that the K-theory misses. Each region of the matrix then refers to particular physical conditions: elements in the main diagonal refer to still fluid and if they are close to one no mixing occurs in that layer, elements close to the main diagonal are influenced by slow mixing upward or downward, while elements far from the diagonal refer to fluid influenced by faster mixing (Figure 5).

TRENDS AND RESULTS

The mixing layer height evolution found using the methods described in the previous section is plotted in Figure 6. The comparison between the two methods shows good agreement. Error bars of z_i are also plotted. They are computed starting from the 90% confidence interval for the vertical velocity standard deviation σ_w based on the sample standard deviation s_w and the chi-square function, and from the 90% confidence interval for the mean temperature μ_T based on the sample mean $\overline{T}$ and t-Student function (Bendat and Pearsol, 1971). The number of independent samples is computed by using the autocorrelation coefficient (Dore et al., 2009b).The evaluation of z_i by using temperature data is statistically more accurate for later times, but it is not for earlier times due to the low number of samples. On the contrary, the velocity-based method is very sensitive to the irregular shape of the standard deviation profiles; this is mainly true for experiment #2, which presents error bars for velocity-based method larger than experiment #1.

The previous analysis allows normalizing the vertical velocity standard deviation profiles accordingly the Deardorff mixed layer similarity (Willis and Deardorff, 1974) by employing the convective velocity, w*, and the mixing layer height, z_i (Figure 7). After normalization, all profiles collapse on the same curve, losing the dependence on time and features of the experiment. The observation of normalized profiles proves that the mixing layer upper limit is located where the standard deviation became about 7% of the maximum value. Once we prove the phenomenon is self similar, that percentage depends neither on experimental conditions nor on time. Our present results are also compared to atmospheric and tank experiments (Lenschow, 1974; Willis and Deardorff, 1974; Lenschow et al., 1980; Deardorff and Willis, 1985; Cenedese and Querzoli, 1994) and field measurements (Young, 1988). The comparison shows a fairly nice agreement, demonstrating the validity of our experimental investigation and its applicability for the study of the real atmospheric boundary layer.

The Deardorff mixed layer similarity was used also to normalize the transilient matrices depicted in Figure 8.

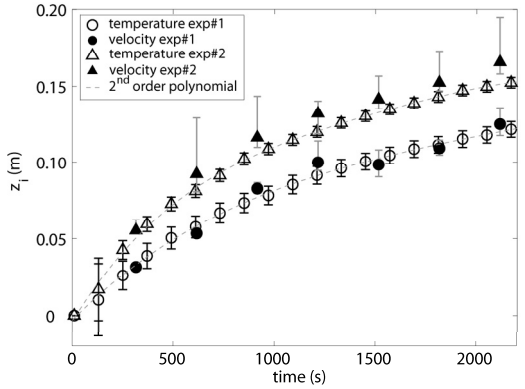

Figure 6. Comparison of the mixing layer height evolution computed by temperature and velocity measurements.

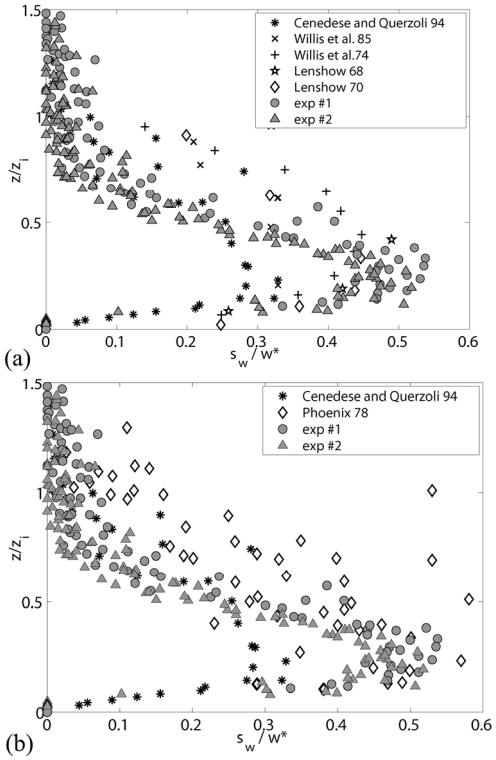

Figure 7. Standard deviation of vertical velocity profiles normalized accordingly the Deardorff mixed layer similarity (Willis and Deardorff, 1974) compared with (a) atmospheric and tank experiments and (b) field measurements.

Each transilient matrix in fact refers to a non-dimensional time interval, being normalization a necessary step for unsteady phenomenon. One can clearly see that at the beginning ($\Delta t^* = 0.01$) all the elements along the main diagonal are close to one, meaning that the fluid is at rest and no mixing occurs. As convection evolves inside the mixing layer the matrices become more and more dispersed showing a faster mixing for greater non-dimensional time lags. For large time lags ($\Delta t^* > 0.4$) tracer spreads out almost uniformly within the mixing layer and the transilient matrix assumes uniform values in that area. Moreover the asymmetry on the contours plot demonstrates that the transport is preferentially downward.

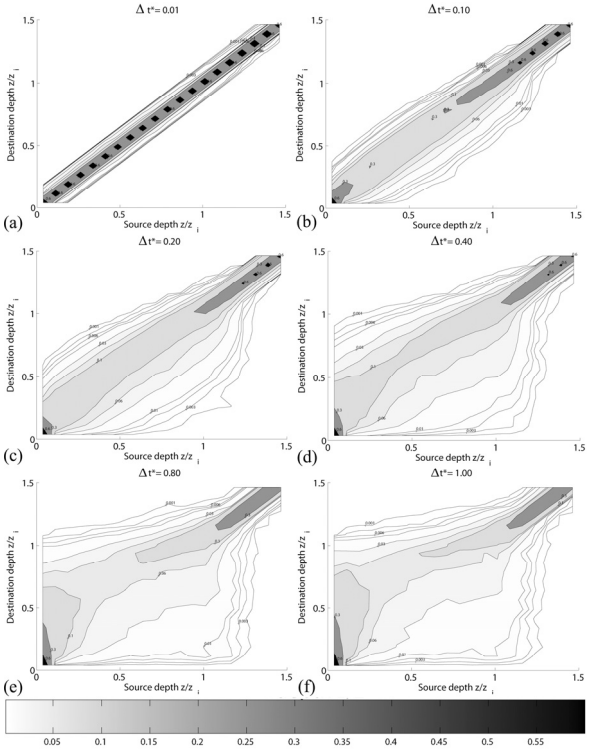

Figure 8. Transilient matrices for various non-dimensional time lags

CONCLUSIONS

The flux through the interface between the mixing layer and the stable layer plays a major role in understanding, characterizing and forecasting the quality of water in stratified lakes and in the upper portion of the oceans and the quality of air in the atmosphere. These issues have motivated our experimental investigation that was aimed at predicting mixing layer growth as a function of initial and boundary conditions and describing the fate of a contaminant dissolved within the fluid phase.

Characteristic structures have been observed in the convective boundary layer: growing domes or turrets presenting an extremely sharp interface at their top, flat regions of large horizontal extent after a dome has spread out or receded, and cusp-shaped regions of entrainment pointing into the convective fluid. Dome characteristic dimensions are of the same order of magnitude as the mixing layer height, while their lifetime is less or equal to the time a fluid particle would need to complete a whole cycle moving through the rising dome and returning in the down-welling region.

There are some phenomena, i.e. pollutant dispersion, that are naturally described in a Lagrangian frame of reference. For a full Lagrangian description, particles have to be tracked for a period of several time scales. The flow under investigation is unsteady in a Lagrangian reference frame since particles, during their motion, reach regions that can be considered homogeneous only in the horizontal plane. The 3D-PTV technique allows long trajectories to be reconstructed within the flow field.

Experimental data demonstrate the validity of Deardorff mixed-layer similarity (Willis and Deardorff, 1974) for the turbulent structure of the boundary layer. Moreover the comparison with literature data shows a very good agreement with measurement taken both at bench and real scale, demonstrating the validity of our experimental task and its applicability for the study of the real atmospheric boundary layer and its monitoring for environmental purposes. The transilient matrix approach (Stull, 1988) allows us to describe in a detailed way the mixing features inside the mixing layer, demonstrating a more and more faster mixing as the time goes on from the onset of convection, with a preferential direction downward.

REFERENCES

Bendat, JS, and Piersol, AG, 1971, *Random data: analysis and measurement procedures*, Wiley-Interscience, New York, London, Sidney, Toronto.

Cenedese, A., and Querzoli, G.,1994, "A laboratory model of turbulent convection in the atmospheric boundary layer", *Atmospheric Environment*, vol. 28, no. 11, pp. 1901-1913.

Deardorff, J.W., 1970, "Convective velocity and temperature scales for the unstable planetary boundary layer and for Rayleigh convection", *J. Atmos. Sci*, vol.27, pp.1211-1213.

Deardorff, JW, and Willis, GE, 1985, "Further results from a laboratory model of the convective planetary boundary layer", *Boundary-Layer Met*, vol. 35, pp. 205-236.

Dore, V, Moroni, M, and Cenedese, A, 2009a, "Investigation of Penetrative Convection in Stratified Fluids through 3D-PTV", *Exp. in Fluids*, (Submitted).

Dore, V, Moroni, M and Cenedese, A, 2009b, "Quantifying mixing in a convective boundary layer", *Heat Trans. Eng.*, (Submitted).

Imberger, J., and Ivey, G.N., 1991, "On the Nature of Turbulence in a Stratified Fluid. Part II: Application to Lakes", *Journal of Physical Oceanography*, vol.21, pp. 659-680.

Kato, H., and Phillips, O.M., 1969, "On the penetration of a turbulent layer into stratified fluid", *J. Fluid Mech*, vol. 37, no. 4, pp.643.

Lenschow, D. H., 1974, "Model of the height variation of the turbulence kinetic budget in the unstable boundary layer", *J. Atmos. Sci.*, vol.31, pp 465-474.

Lenschow, D. H., Wyngaard, J.C., and Pennel , W.T., 1980, "Mean-field and second moment budgets in a baroclinic, convective boundary layer", *J. Atmosl. Sci.*, vol. 31, pp 465-464.

Miesch, M.S., Brandenburg, A., and Zweibel, E.G., 2000, "Nonlocal transport of passive scalars in turbulent penetrative convection", *Physical Review*, vol. E 61,No.1, pp. 457-467.

Stull, RB, 1988, *An introduction to boundary layer meteorology,* Kluwer Academic Publishers, Dordrecht, Boston, London.

Willis, G.E., and Deardorff, J.W., 1974, "A laboratory model of the unstable planetary boundary layer", *J. Atmos. Sci.*, vol.31, pp1297-1307.

Young, G.S, 1988, "Turbulence structures of the convective boundary layer. Part I: variability of normalized turbulence statistics", *J. Atmos. Sci*., vol.45, pp720-726.